



Article

Germination Kinetics and Chlorophyll Fluorescence Imaging Allow for Early Detection of Alkalinity Stress in *Rhododendron* Species

Shusheng Wang^{1,2,3,*}, Leen Leus², Peter Lootens², Johan Van Huylenbroeck²
and Marie-Christine Van Labeke^{1,*}

¹ Department of Plants and Crops, Faculty of Bioscience Engineering, Ghent University, 9000 Ghent, Belgium

² Plant Sciences Unit, Flanders Research Institute for Agriculture, Fisheries and Food (ILVO), 9090 Melle, Belgium

³ Lushan Botanical Garden, Chinese Academy of Sciences, Jiujiang 332900, China

* Correspondence: wangss@lsbg.cn (S.W.); mariechristine.vanlabeke@ugent.be (M.-C.V.L.)

Abstract: *Rhododendron* species are typical calcifuges that do not grow well in calcareous soils characterized by alkaline pH and high concentrations of Ca^{2+} . In this study, we investigated the effects of three pH levels and a Ca^{2+} treatment on the in vitro germination and seedling growth of three *Rhododendron* species: *R. chihsinianum*, *R. fortunei*, and *R. vernicosum*. Alkaline pH had no significant effect on germination parameters (g_{MAX} , mean germination time and germination uniformity) but significantly increased abnormal leaf development (AL) and mortality in all three species. Adding extra Ca^{2+} reduced the mean germination time for *R. vernicosum*. The negative influence of alkaline pH on seedlings was already visible on the second day of treatment as measured by chlorophyll fluorescence imaging parameters (F_v/F_m and Φ_{PSII}) on *R. fortunei*. Extra Ca^{2+} alleviated the negative effect of alkaline pH and increased F_v/F_m 41 days after seed germination in *R. fortunei* and *R. chihsinianum* and reduced mortality for all three species. In conclusion, alkaline pH mainly influenced seedling development and growth but not the germination process itself. Chlorophyll fluorescence imaging can be an efficient way to perform high-throughput in vitro screening of *Rhododendron* seedlings for alkalinity tolerance.

Keywords: *Rhododendron*; pH; calcium; germination; leaf chlorosis; mortality; chlorophyll fluorescence imaging



Citation: Wang, S.; Leus, L.; Lootens, P.; Van Huylenbroeck, J.; Van Labeke, M.-C. Germination Kinetics and Chlorophyll Fluorescence Imaging Allow for Early Detection of Alkalinity Stress in *Rhododendron* Species. *Horticulturae* **2022**, *8*, 823. <https://doi.org/10.3390/horticulturae8090823>

Academic Editors: Yoon Jin Kim and Byoung Ryong Jeong

Received: 22 August 2022

Accepted: 5 September 2022

Published: 7 September 2022

Publisher's Note: MDPI stays neutral with regard to jurisdictional claims in published maps and institutional affiliations.



Copyright: © 2022 by the authors. Licensee MDPI, Basel, Switzerland. This article is an open access article distributed under the terms and conditions of the Creative Commons Attribution (CC BY) license (<https://creativecommons.org/licenses/by/4.0/>).

1. Introduction

Rhododendron is one of the largest plant genera with nearly 1000 species, of which 571 occur in China [1]. Abundant genetic variation exists due to either introgression through natural hybridization [2,3] or controlled cross-breeding [4]. *Rhododendrons* are cultivated globally, but their garden applications are mainly restricted to native or amended acidic soils because of their low tolerance to calcareous soil conditions. They are typically calcifuges (lime intolerant) plants, which prefer soils between pH 4.5–6.0 and cannot grow well on lime/calcareous soils [5]. Bicarbonate ion toxicity and iron deficiency have both been described as detrimental to calcifuge plants. Soils with a high lime content may contain high bicarbonate (HCO_3^-) concentrations in their soil solution. This can inhibit cell elongation and thus root length in non-adapted calcifuges and disrupt the ion uptake [6]. A recent study reported that the high pH linked to the strong buffering capacity of HCO_3^- is the key factor that determines whether calcifuge *Lupinus* species can survive in calcareous soils [7].

The root–soil interface (root exudates, rhizosphere microorganisms, and mycorrhizae) also plays an important role in the mineral nutrition of lime-intolerant plants [8–10]. The solubility of Fe oxides is exceedingly low above neutral pH; therefore alkaline soils have low plant-available iron which will lead to iron deficiency chlorosis in *Rhododendron* and

finally plant death [11]. Higher plants employ rhizosphere acidification as a strategy to reduce Fe(III) and subsequent uptake of Fe(II) [12,13]. Therefore lime intolerance has often been related to the inability of plants to solubilize adequate amounts of Fe from high pH soils or an inability to retain Fe as an active metabolite in plant tissues [14].

High levels of calcium as such do not suppress *Rhododendron* growth [15]. The major factor limiting *Rhododendron* growth in calcareous soils is the increase in pH, rather than an increase in the concentration of calcium ions [16]. Ca^{2+} controls diverse intracellular processes and impacts nearly every aspect of cellular life [17]. Ca^{2+} is involved in the regulation of plant responses to both biotic and abiotic stress. Cytosolic free calcium is central to the response to these stresses although its role is hardly investigated concerning nutrient deprivation or alkaline stress [18]. Kerchev et al. [19] reviewed priming agents that are used to trigger natural defense mechanisms in plants including pretreatment of crops with calcium. In addition in *Rhododendron*, an exogenous leaf application with calcium chloride effectively alleviates chlorophyll decline under heat stress [20].

Contrary to most of the members of this genus, some rhododendrons can thrive in alkaline soils. *Rhododendron* species surviving in limestone habitats have recently been described [21]. In addition, Wang et al. [22] proposed a list of lime-tolerant *Rhododendron* taxa based on geocoding of herbarium species in locations with the topsoil pH above 7.2 and $\text{CaCO}_3 > 2\%$. Although it has been suggested that rhododendrons achieve this adaptation through high pH avoidance mechanisms, other research suggests that they are in fact lime-tolerant species with roots penetrating calcareous soils and growing in the same locations as other native calcicole taxa [5].

Increased abiotic stress tolerance can be gained through natural or artificial selection [23]. Seed germination and early seedling growth are the most sensitive stages for abiotic stress conditions in the majority of plant species [24]. In vitro seed germination can be useful for speeding up the breeding cycle by improving germination percentage, shortening germination time, and enhancing seedling growth [25]. It is also helpful for setting up a standardized bio-assay where adding a stress factor to the germination medium could help to select more tolerant genotypes. Combining this approach with non-invasive screening methods could help to select the desired traits. Chlorophyll fluorescence imaging (CFI) is a powerful and fast technique to detect stress at the plant level. It can also determine the intra-plant variation and can be used in high-throughput phenotyping systems [26,27]. CFI has been increasingly used for screening tolerant genotypes as well as sensing and early detection of biotic or abiotic stress [28–31].

The availability of more lime-tolerant *Rhododendron* genotypes would broaden the market due to a reduced need for soil amendment if they are used as rootstocks or as an interesting gene pool in breeding programs. In this respect, *Rhododendron* species surviving in habitats with lime soil are valuable genetic resources for breeding for lime tolerance [22].

The objectives of our study were (1) to investigate the effects of bicarbonate/high pH on germination and early seedling growth of three *Rhododendron* species *R. fortunei*, *R. vernicosum*, and *R. chihsinianum* in light of their different lime tolerances. In their natural habitats in China, the topsoil for both *R. fortunei* and *R. vernicosum* ranges from median/upper quartile values of 6.5/7.8 and 6.5/8, respectively, while lower pH ranges were found for *R. chihsinianum* (pH 5/6.5) [22]; (2) to investigate if exogenous calcium supply protects rhododendrons from the adverse effects of alkaline stress; and (3) to develop a high-throughput phenotyping method for screening of tolerant genotypes at seedling stage using chlorophyll fluorescence imaging.

2. Materials and Methods

2.1. Plant Materials

Seeds of *R. fortunei*, *R. vernicosum*, and *R. chihsinianum* were collected in November 2016 from Lushan Botanical Garden (29° 51' N, 115° 59' E), Chinese Academy of Sciences, Jiujiang, China, and stored at room temperature.

2.2. Culture Media

Two media based on the Anderson medium [32] were used, one for seed germination (Exp 1 and 3) and one for the seedling response (Exp 2).

The seed germination medium: 2 g L⁻¹ Anderson's *Rhododendron* (Duchefa, The Netherlands), 30 g L⁻¹ sucrose, and 6 g L⁻¹ agar (International Diagnostics Group plc, Lancashire, UK) were dissolved in distilled water, and pH was adjusted to 5.4 before autoclaving. The Anderson medium contains 2.99 mM CaCl₂. After autoclaving, the pH of the medium was adjusted to three different pH levels by adding NaHCO₃ and to two calcium levels by adding CaCl₂·2H₂O using filter sterilization (Table 1). The medium was poured into Petri dishes (diameter 5 cm). After solidification, the pH of one randomly selected Petri dish per treatment was determined using a flat pH electrode (pH meter MU6100L, pH electrode SF113, VWR, Darmstadt, Germany). A second pH measurement was performed at the end of the experiment, measuring all plates.

Table 1. Experiment 1: Overview of the medium pH after autoclaving at the start of and after 90 days (end of the experiment). The pH of the media decreased by around 1 unit, but the pH gradient was maintained. Treatment 1 is the control medium for seed germination and seedling development.

Treatment	NaHCO ₃ (mM)	CaCl ₂ ·2H ₂ O (mM)	pH	
			Day 0	Day 90 (Mean ± SE, n = 4)
1 Acidic	0	0	5.7 *	4.5 ± 0.06
2 Neutral	2	0	6.7	5.5 ± 0.04
3 Alkaline	10	0	7.5	7.0 ± 0.08
4 Acidic + Ca ²⁺	0	3.4	5.6	4.4 ± 0.03
5 Neutral + Ca ²⁺	2	3.4	6.7	5.3 ± 0.07
6 Alkaline + Ca ²⁺	10	3.4	7.3	6.3 ± 0.18

(*) pH before autoclaving was 5.4; autoclaving resulted in a small pH increase based on the pH measurement of the solidified medium.

After the preparation of the media, the germination tests were set up in six treatments with three initial pH levels measured on the solidified medium: acidic (5.6–5.7), neutral (6.72–6.74), alkaline (7.3–7.5), and two Ca levels (control and supplemental 3.4 mM Ca) (Table 1).

The medium for seedling response: 2 g L⁻¹ Anderson's *Rhododendron*, 30 g L⁻¹ sucrose, 1 mg L⁻¹ IAA, 4 mg L⁻¹ 2-IP, and 7 g L⁻¹ agar were dissolved in distilled water, with pH adjusted to 5.4. After autoclaving, the medium was added to sterile 24-well plates with 1 mL medium per well. To determine the initial pH after solidification, the medium was also poured into Petri dishes (diameter 5 cm) to measure the pH, and at the end of the experiments, the pH of the media was measured in all the well plates using a pH meter MU6100L as mentioned above.

2.3. In Vitro Growing Conditions

For all three experiments, plants were kept in a growth chamber at 21 °C and were placed on a bottom cooling system set at 19.5 °C to avoid condensation in the plates. A 16 h photoperiod with a photon flux density (PPFD) of 50 µmol·m⁻²·s⁻¹ was provided by cool-white fluorescent lamps.

2.4. Experimental Setup

2.4.1. Experiment 1

In March 2017, the 4-month-old stored seeds of *R. fortunei* were sown in vitro on the germination media (Table 1) with 25 seeds per dish and 4 repeats per treatment. Before sowing, seeds were surface sterilized for 1 min in 70% ethanol, 15 min in sodium hypochlorite (1% bleach), then rinsed in sterile distilled water for 1, 5, and 10 min, respectively.

2.4.2. Experiment 2

In July 2017, seedlings in the first true leaf stage were selected for uniformity from the treatment: acidic + Ca^{2+} (the highest seedling quality of experiment 1) and transplanted into 24-well plates filled with the seedling response medium. After acclimation for 25 days, 4 pH treatments were applied using NaHCO_3 (see Table 2). For each treatment, 16 repeats (4 wells \times 4 plates) were performed. The pH of the medium in all wells was measured at the end of the experiments (21 DAS).

Table 2. Overview of the bicarbonate treatments in experiment 2 and medium pH 21 days after the start of the treatment (21 DAS). (Mean \pm SE, $n = 16$).

pH Before Autoclaving	Treatment (0.1 mL/Well)	Target HCO_3^- (mM) in the Medium	pH at 21 DAS
5.4	distilled H_2O	0	6.2 \pm 0.05
5.4	50 mM NaHCO_3	4.5	7.0 \pm 0.02
5.4	150 mM NaHCO_3	13.6	8.2 \pm 0.05
5.4	250 mM NaHCO_3	22.7	8.9 \pm 0.02

2.4.3. Experiment 3

In August 2017, 9-month-old stored seeds of *R. fortunei*, *R. vernicosum*, and *R. chihsinianum* were sterilized as described in experiment 1 and sown on the 6 germination media (see experiment 1) with 25 seeds per dish and 5 dishes per treatment. The sterilization protocol was the same as in experiment 1.

2.5. Measurements

2.5.1. Germination and Seedling Growth (Experiments 1 and 3)

Seeds with radicle emergence ≥ 1 mm were considered germinated, and the number of germinated seedlings was daily recorded. Maximum germination (g_{MAX}), mean germination time (MGT), and the time between 25% and 75% germination (uniformity) were calculated using the curve fitting module of ‘Germinator’ [33].

The number of seedlings with open cotyledons (CO) and abnormal cotyledon/leaf morphology (AL; yellow or discolored) were recorded daily up to two months after sowing in experiment 1 and experiment 3. The number of seedlings with true leaves (TL) and mortality were recorded daily up to three months after sowing in experiment 1 and experiment 3.

2.5.2. Chlorophyll a Fluorescence Imaging (Experiments 2 and 3)

Chlorophyll a fluorescence images were obtained using a FluorImager chlorophyll fluorescence imaging system (Technologica Ltd., Colchester, UK). Before the experiment, a preliminary study was performed to determine the optimal protocol for acquiring kinetic chlorophyll fluorescence images. The maximum quantum efficiency of the photosystem II (F_v/F_m) was measured after 20 min of dark adaptation using a saturating light pulse with a photosynthetic photon flux density (PPFD) of 6000 $\mu\text{mol m}^{-2} \text{s}^{-1}$ for 1 s. Plantlets were exposed to actinic light of 40 $\mu\text{mol m}^{-2} \text{s}^{-1}$ from then on. Saturating flashes were applied every 30 s six times, and the effective quantum efficiency of PSII (Φ_{PSII}) after 3 min of light adaption was used for data analysis. In experiment 2, chlorophyll fluorescence images were analyzed from day 0 (the day before the treatment) to day 10 at daily intervals and finally at day 21 through closed lids of the 24-well plates. In experiment 3, chlorophyll fluorescence images were taken at 41 (seeds germinated and cotyledons visible) and 61 days after placing the seeds on the media through the closed lids of the Petri dishes. The same variables were evaluated in experiments 2 and 3.

2.6. Statistical Analysis

All statistical tests were performed in SPSS Statistics Software 25.0 (SPSS, Chicago, IL, USA). The homogeneity of variances was tested by Levene’s test ($p = 0.05$). Data were

analyzed using one-way or two-way ANOVA, followed by Tukey's HSD test ($p = 0.05$). The non-parametric Kruskal–Wallis analysis was used for the main effects (pH or Ca^{2+}) when heteroscedasticity of variances was present, followed by the Mann–Whitney U test with Bonferroni correction ($p = 0.05$).

3. Results

3.1. Experiment 1

The seeds of *R. fortunei* started to germinate 12 days after sowing, and germination continued until day 35 (Figure S1). The pH had no significant effect on the germination kinetics as assessed by g_{MAX} , MGT, and uniformity (Table 3). The germination rate was high (>74%), and the mean germination time (MGT) varied between 17–19.5 days (Table 3). Adding extra Ca^{2+} significantly increased MGT ($p < 0.01$). Only for germination uniformity, a significant interaction between pH and Ca^{2+} ($p < 0.05$) was present (Table 3).

Table 3. Effects of pH and additional 3.4 mM Ca^{2+} on maximum germination (g_{MAX}), mean germination time (MGT), the time between 25% and 75% germination (uniformity), and on seedling development and mortality expressed as a percentage of the number of germinated seeds (CO—open cotyledons, TL—true leaves, AL—abnormal cotyledons or leaves) in *Rhododendron fortunei*. All values are mean \pm SE, $n = 8$ for pH, $n = 12$ for Ca^{2+} .

	Germination Parameters on Day 35			Seedling Performance on Day 60			Seedling Performance on Day 90	
	g_{MAX} (%)	MGT (Day)	Uniformity (Day)	CO (%)	TL (%)	AL (%)	TL (%)	Mortality (%)
pH								
Acidic	74.0 \pm 5.8	17.7 \pm 0.5	6.2 \pm 0.4	96.5 \pm 1.3	18.6 \pm 5.0	0.0 \pm 0.0 b	37.0 \pm 5.2	0.6 \pm 0.7 b
Neutral	77.5 \pm 5.7	18.2 \pm 0.7	5.2 \pm 0.7	98.1 \pm 0.9	24.7 \pm 5.4	0.0 \pm 0.0 b	49.0 \pm 6.6	1.1 \pm 0.7 b
Alkaline	77.5 \pm 7.0	18.5 \pm 0.6	5.6 \pm 0.5	98.7 \pm 0.8	34.0 \pm 5.6	43.6 \pm 10.7 a	47.6 \pm 4.0	39.0 \pm 9.4 a
Ca^{2+}								
0	78.7 \pm 4.8	16.8 \pm 0.4	5.5 \pm 0.5	97.1 \pm 0.9	31.7 \pm 4.5	18.2 \pm 7.8	51.7 \pm 4.9	19.3 \pm 8.2
3.4 mM	74.0 \pm 5.1	19.5 \pm 0.3	5.9 \pm 0.4	98.4 \pm 0.6	19.8 \pm 4.0	10.8 \pm 7.8	37.4 \pm 2.9	10.9 \pm 6.9
Anova								
pH	ns	ns	ns	ns	ns	***	ns	**
Ca^{2+}	ns	**	ns	ns	*	ns	*	ns
Interaction	ns	ns	*	ns	ns	ns	ns	ns

ns, *, **, or *** indicate non-significant or significant effects at $p < 0.05$, 0.01, or 0.001 according to a 2-way ANOVA or a non-parametric Kruskal–Wallis analysis (AL and mortality); a, b denote significant differences according to Tukey's HSD test or the Mann–Whitney U test (AL and mortality) ($p = 0.05$).

The cotyledons began to open around day 21 up to day 40. The true leaves emerged around day 38 in media with extra Ca^{2+} and day 41 without extra Ca^{2+} (Figure S1). The development of cotyledons (CO) and true leaves (TL) was not influenced by pH, but an alkaline pH had a highly significant effect on the occurrence of yellow cotyledons/leaves (AL) ($p < 0.001$) and seedling mortality ($p < 0.01$). Around 25 days after germination (day 60 of the experiment), seedlings in the alkaline medium had a high rate of AL (43.6%) with no AL noted in acidic and neutral medium. One month later (day 90), a high percentage of these seedlings died leading to 39.5% mortality for the alkaline medium, while hardly any seedling loss was noted for the acidic (0.6%) and neutral (1.1%) medium (Table 3).

Extra Ca^{2+} did not significantly affect CO, AL, and mortality, although for CO and mortality, a tendency to lower losses is present. In contrast, extra Ca^{2+} significantly ($p < 0.05$) retarded the development of true leaves compared to media without extra Ca^{2+} (Table 3). No interaction between pH and Ca^{2+} was found for the seedling performance parameters.

3.2. Experiment 2

Chlorophyll *a* fluorescence images were measured for 21 days (Figure 1). F_v/F_m of the control *R. fortunei* seedlings was relatively steady and ranged from 0.519 ± 0.022 before the start of the treatment to 0.525 ± 0.015 on day 21 (Figure 2). However, alkaline pH negatively

influenced F_v/F_m soon after the start of the treatment, with values (mean \pm SE) decreasing from 0.539 ± 0.025 to 0.294 ± 0.042 at pH 8.2 and from 0.470 ± 0.022 to 0.244 ± 0.045 at pH 8.9 on day 1 and day 21, respectively (Figure 2). The negative effects of an alkaline pH were already present after two days for pH 8.9 and after three days for pH 8.2 (Figure 2). Six days after the start of the treatments, F_v/F_m remained significantly low and stable in both pH 8.2 and 8.9. F_v/F_m of seedlings under neutral pH tended to a slight but non-significant decrease compared to the control. Box plots (Figure 3) indicate that at day 21 the median for F_v/F_m decreased, and as pH increased, higher variability in the seedling population was observed, including an increasing number of outliers.

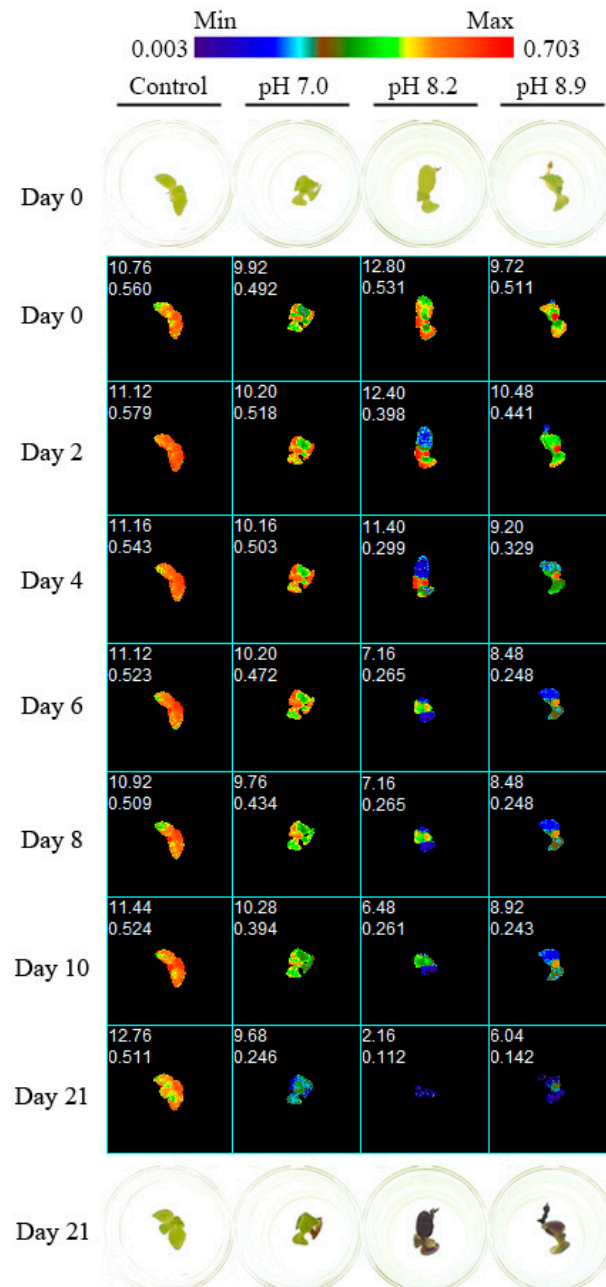
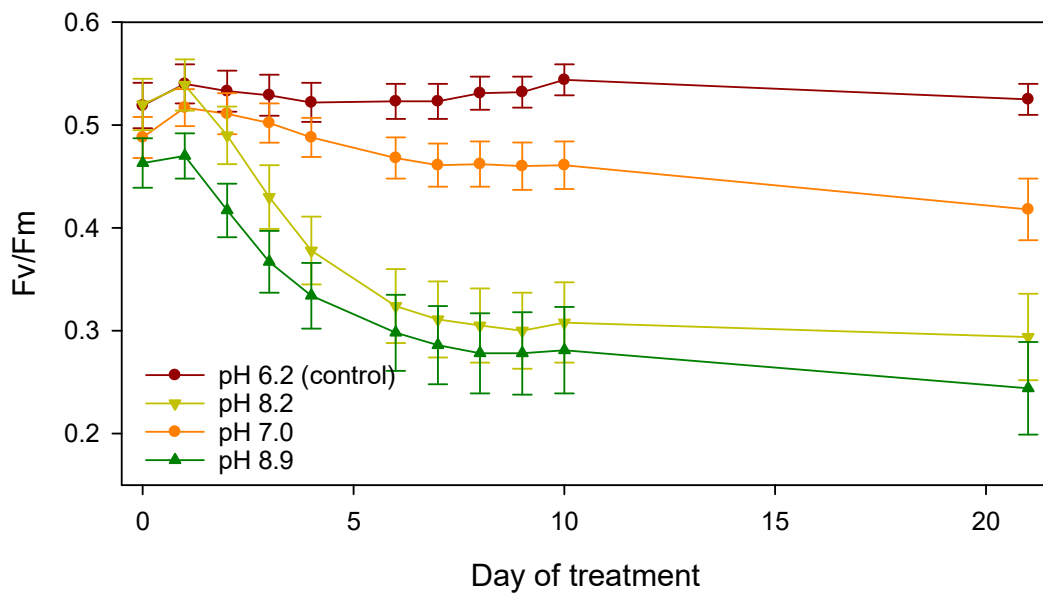


Figure 1. Dynamics of F_v/F_m over time for four *R. fortunei* seedlings subjected to increasing pH treatments (control – pH 6.2, pH 7.0, pH 8.2, pH 8.9). For days 0 and 21, RGB images are shown. Values in the upper left corner of the chlorophyll fluorescence images are the projected area in pixels and the mean F_v/F_m of the seedling in the well.



Parameter	Treatment	Day 0	Day 1	Day 2	Day 3	Day 4	Day 6	Day 7	Day 8	Day 9	Day 10	Day 21
Fv/Fm	Control (pH 6.2)	a	a	a	a	a	a	a	a	a	a	a
	pH 7.0	a	a	a	ab	ab	ab	ab	ab	a	ab	ab
	pH 8.2	a	a	ab	bc	bc	bc	bc	bc	b	b	b
	pH 8.9	a	a	b	c	c	c	c	c	b	b	b

Figure 2. Time series of F_v/F_m (mean \pm SE) of *R. fortunei* seedlings in response to different pH treatments. Different lower-case letters denote significant differences within a day according to Tukey’s HSD test (day 0–3) or the Mann–Whitney U test (day 4–day 21) at $p = 0.05$.

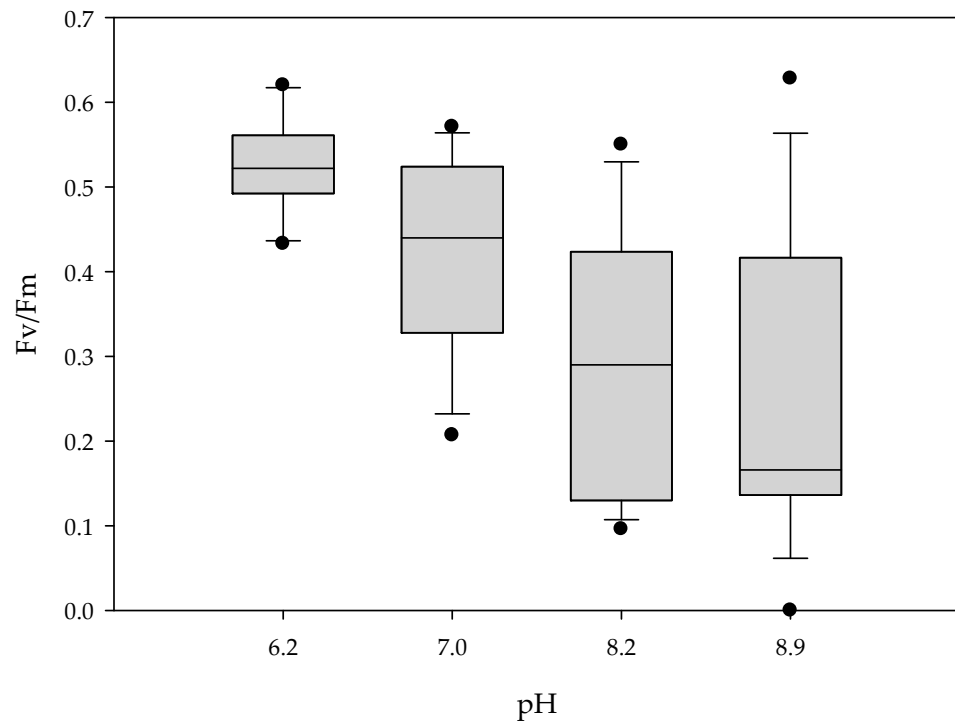
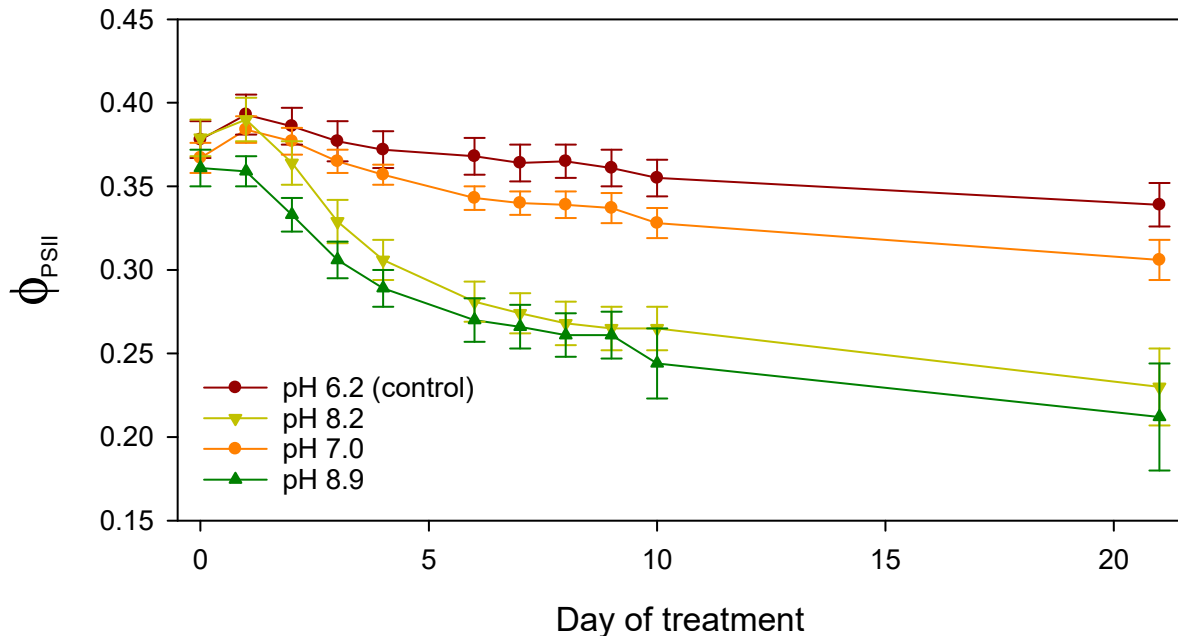


Figure 3. Box plot showing F_v/F_m in response to different pH levels 21 days after the start of the treatment of *R. fortunei* seedlings ($n = 16$) (Exp 2).

The Φ_{PSII} of the seedlings decreased from 0.393 ± 0.012 to 0.339 ± 0.013 in the control and from 0.384 ± 0.008 to 0.306 ± 0.012 at pH 7.0 on day 1 and day 21, respectively. However, during this period the Φ_{PSII} decreased rapidly from 0.390 ± 0.013 to 0.230 ± 0.023 at

pH 8.2 and from 0.359 ± 0.009 to 0.212 ± 0.032 at pH 8.9 (Figure 4). Starting from day 2, the Φ_{PSII} at pH 8.9 was significantly lower than the control (Figure 4). Four days after the start of the treatments, both alkaline pH treatments showed a significantly lower Φ_{PSII} than the control and the neutral pH. The Φ_{PSII} at pH 7.0 did not differ from the control at any of the recorded time points (Figure 4).



Parameter	Treatment	Day 0	Day 1	Day 2	Day 3	Day 4	Day 6	Day 7	Day 8	Day 9	Day 10	Day 21
Φ_{PSII}	Control (pH 6.2)	a	a	a	a	a	a	a	a	a	a	a
	pH 7.0	a	a	a	ab	a	a	a	a	a	a	ab
	pH 8.2	a	a	ab	bc	b	b	b	b	b	b	b
	pH 8.9	a	a	b	c	b	b	b	b	b	b	b

Figure 4. Time series of Φ_{PSII} (mean \pm SE) of seedlings in the treatments of control (pH 6.2), pH 7.0, pH 8.2, and pH 8.9 from day 0 (before the treatment) until day 21. Different lower-case letters denote significant differences within a day according to Tukey’s HSD test (day 0–day 20) or the Mann–Whitney U test (day 21) at $p = 0.05$.

3.3. Experiment 3

In all six treatments, acidification of the media occurred during the experiment of all three species (Table S1), but between treatments, pH differences were maintained. The acidification of the initial neutral pH of 6.8 resulted in a lower pH (5.3 to 5.8) at day 92, for the initial alkaline pH a change to neutral pH (6.8 to 7.3) was observed, and for the acidic pH of 5.6 a change to 4.3 to 4.5.

The seeds of three *Rhododendron* species started to germinate around 14 days after sowing, and germination continued until day 41. Then g_{MAX} , MGT, and uniformity were calculated. For all three species, pH did not significantly affect the germination parameters (g_{MAX} , MGT, and uniformity) and two seedling parameters (CO and TL) (Table S1). The germination of *R. fortunei* was high (g_{MAX} 68–73%) and similar to experiment 1, but the 2 other species had a relatively low germination rate (g_{MAX} 30–40%). Yet MGT did not differ between the species and averaged 21.3 days, nor did the uniformity of germination (6.7 days between 25–75% germination) differ. However, AL and mortality ($p < 0.001$) did significantly increase in the alkaline medium.

Supplementing 3.4 mM extra Ca^{2+} resulted in a species-dependent effect (Table S2). The germination (g_{MAX}) was not affected in *R. chihsinianum* and *R. vernicosum*, but extra Ca^{2+} increased g_{MAX} by 10% for *R. fortunei* ($p < 0.05$). Mean germination time decreased significantly by 2.5 days ($p < 0.001$) for *R. vernicosum* but not for the other species. Although

MGT was not affected for *R. fortunei*, a significant ($p < 0.01$) higher uniformity of germination was noted with extra Ca^{2+} ; it took 5.6 days between 25% and 75% germination of seeds compared to 7 days if no extra Ca^{2+} was given.

Cotyledon (CO) and leaf development (TL) was not influenced by extra Ca^{2+} . Overall, extra calcium did reduce leaf yellowing (AL) and mortality significantly for *R. fortunei* but not for the other species. However, a significant interaction ($p < 0.01$) between pH \times Ca was found for mortality for all three species. Adding calcium to the alkaline medium reduced the mortality for all species, but this decrease was strongly present for *R. fortunei* (Table S2). The mortality in alkaline medium with extra Ca^{2+} ranged from 5.6% for *R. fortunei* to 26.7% for *R. chihsinianum* and 34.4% for *R. vernicosum*. If no extra calcium was given, the mortality in the alkaline medium ranged from 50.8% for *R. fortunei* to 52.8% for *R. chihsinianum* and 72.7% for *R. vernicosum* (Figure 5).

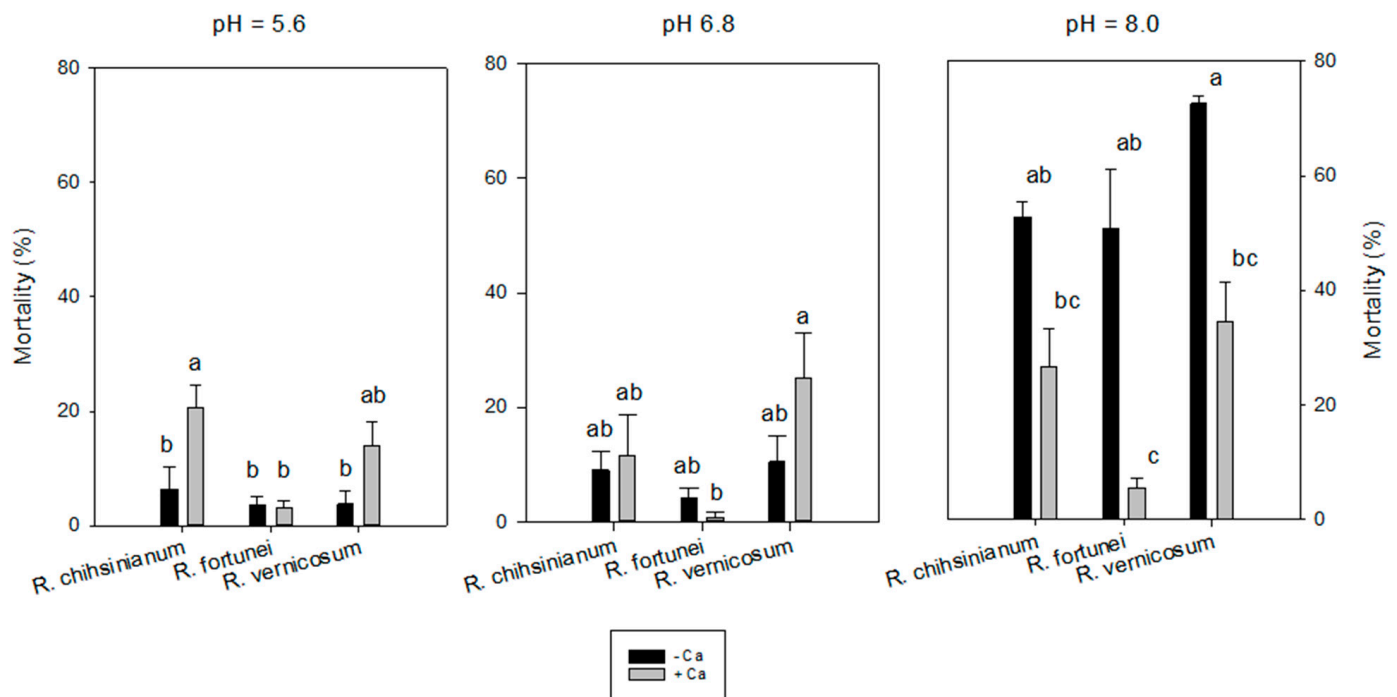


Figure 5. Mortality of three *Rhododendron* sp. at different pH and with/without additional calcium. Mean \pm SE, $n = 5$ —a,b,c indicate significant differences according to Tukey's HSD test for each pH level.

The functioning of the photosynthetic apparatus was investigated by CFI (Table S2, Figures 6 and 7). An alkaline medium pH resulted for all three species on day 41 and day 61 in a significant decrease of both F_v/F_m and Φ_{PSII} ($p < 0.001$) (except for *R. chihsinianum* only a negative trend was observed for Φ_{PSII} on day 61) (Table S2). Extra Ca^{2+} significantly enhanced F_v/F_m on day 41 in *R. chihsinianum* and *R. fortunei*, but this initial positive effect was gone on day 61. Extra Ca^{2+} did not affect Φ_{PSII} . A significant interaction between pH and extra Ca^{2+} was observed for *R. chihsinianum* and *R. vernicosum*, whereby the effect of calcium is limited at pH 5.6 and 6.8 but significant (or strong tendency) at pH 8 (Figure 7). It is also clear that F_v/F_m does not differentiate between the species for a given pH and Ca^{2+} level (Figure 7).

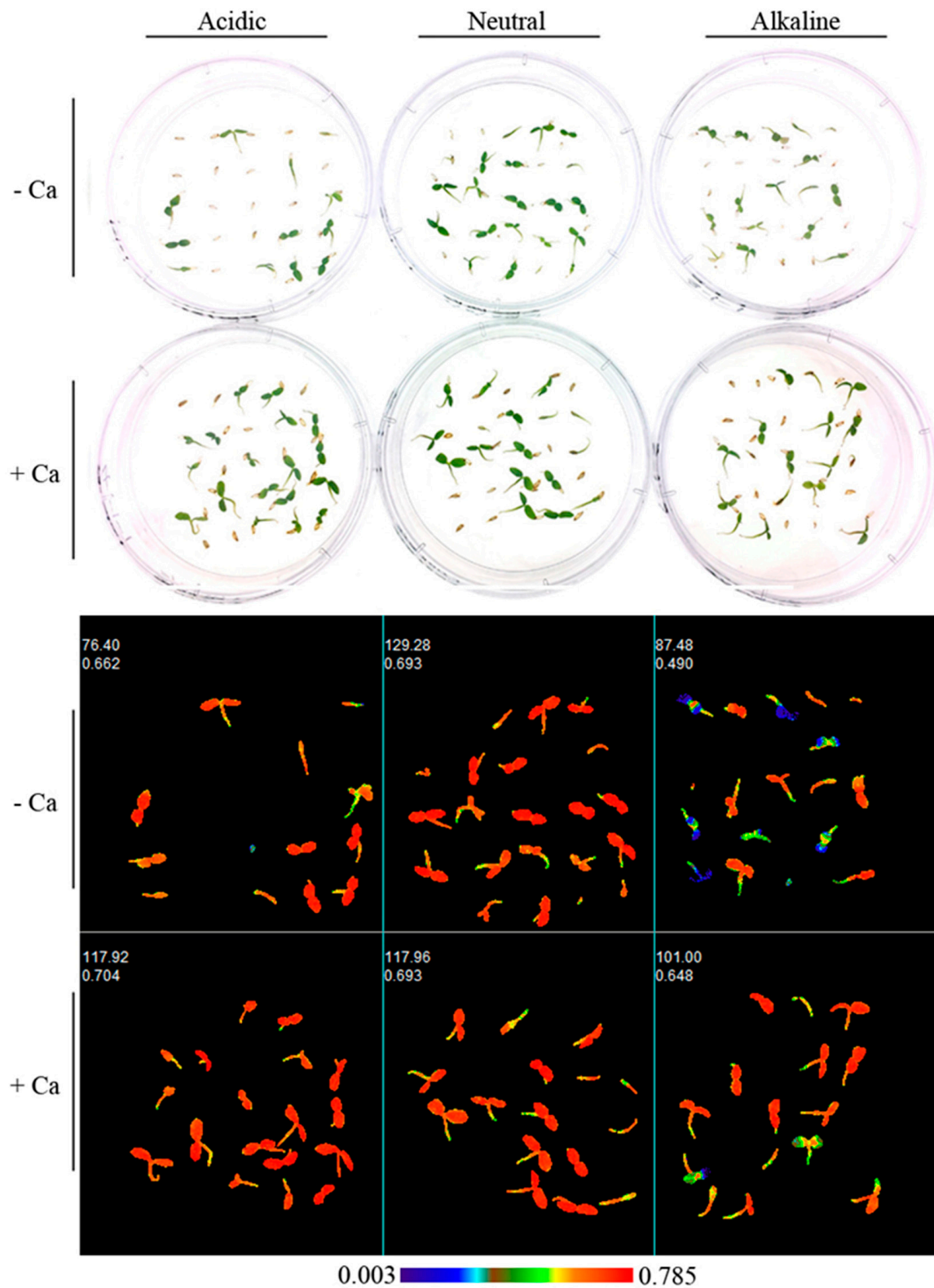


Figure 6. RGB images and F_v/F_m images on day 41 of *R. fortunei* in 6 treatments (acidic, neutral, alkaline, acidic + Ca^{2+} , neutral + Ca^{2+} , alkaline + Ca^{2+}). Values in the upper left corner of the chlorophyll fluorescence images are the projected area in pixels and mean values of F_v/F_m of all seedlings in one petri dish.

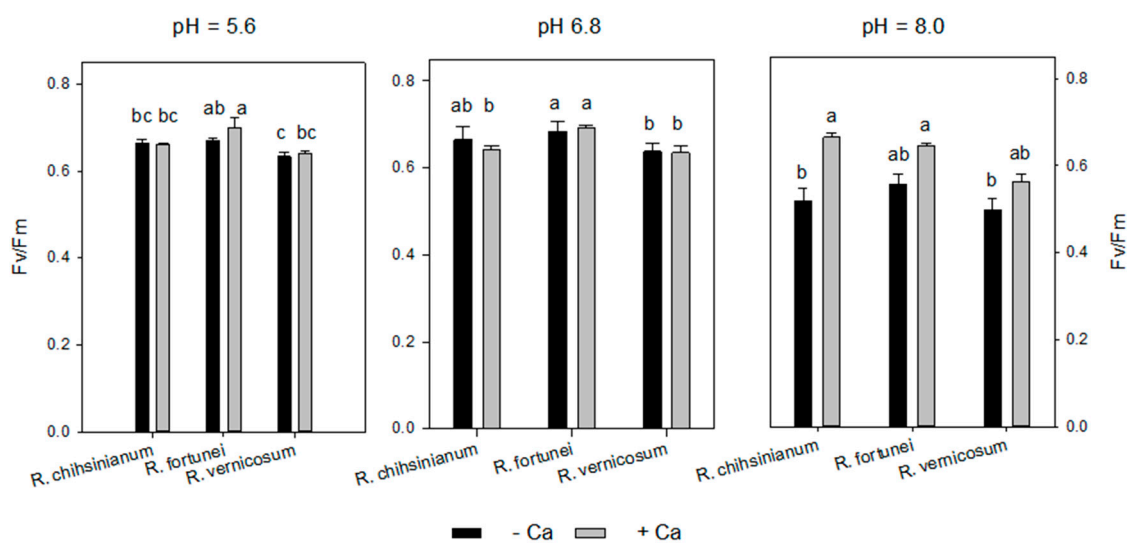


Figure 7. F_v/F_m of three *Rhododendron* sp. at different pH and additional calcium at day 41. Mean ± SE, $n = 5$ —a,b,c indicate significant differences according to Tukey's HSD test for each pH level.

4. Discussion

Rhododendron is generally known as a calcifuge that prefers moderate acidic soil. Nonetheless, intra-species variation in tolerance to alkaline soils exists in this genus as shown in the study of Wang et al. [22]. Although in many regions soil salinization and alkanization co-occur, we focus here on the reaction of three *Rhododendron* species to high pH (alkaline stress) during their early stages of development. Two of the studied species, *R. fortunei* and *R. vernicosum*, were reported to be less sensitive to calcium carbonate [34] or high pH [22,35]. Furthermore, *R. fortunei* was considered to be a promising species in breeding for lime-tolerant rhododendrons [36] and is one of the parents of the lime-tolerant INKARHO[®] rootstocks developed in Germany [37].

The seed germination of the three *Rhododendron* species was not affected by pH as shown by the in vitro germination experiments (Tables 3 and S2). The speed of seed germination depends on the speed of water uptake. The applied alkaline stress of 10 mM NaHCO₃ (pH 7.3–7.5) did not inhibit water uptake. In addition, Yu et al. [38] found no negative effects of an alkaline stress concentration of 30 mM NaHCO₃ on the germination rate of common bean, while 60 mM NaHCO₃ delayed the germination.

Once germination took place and the roots started to absorb nutrients, the first adverse effects of high pH on seedling development appeared. The higher pH of the alkaline medium may have seriously reduced the availability of mineral nutrients (precipitation) or loss of root function (absorption), leading to a higher percentage of leaf yellowing (AL). These AL seedlings were not able to survive for a longer period in the alkaline medium as indicated by high mortality at day 90 (Tables 3 and S2). Yet, mortality differences between the species were not very pronounced (Figure 5, Table S2). This may be due to an acidification effect of the roots. Indeed, we found that a pH decrease in the root zone occurred for all tree species towards pH neutral levels though *R. fortunei* roots tended to have a higher adjustment ability (Table S1) and also hardly any mortality if extra calcium was added (Figure 5).

In beans, under alkaline stress of 30–60 mM NaHCO₃, Ca²⁺ ions are closely related to alkaline salt tolerance [38], but this effect disappeared at higher concentrations NaHCO₃. Guo et al. [39] found that wheat under alkali stress (80 mM NaHCO₃/Na₂CO₃—pH 9) enhances the Ca²⁺ content in the roots, and this will trigger the SOS–Na excluding system leading to lower sodium accumulation in the shoots and thus leaf damage. In our research, an extra 3.6 mM Ca²⁺ (supplied as CaCl₂) counteracted certain adverse effects of a higher pH, although differences between species were detected (Table S2). The

calcifuge *R. chihsinianum* hardly responded to extra Ca^{2+} during seed germination and early seedling growth. Extra Ca^{2+} significantly enhanced the final seed germination (g_{MAX}) and germination uniformity but did not affect the germination speed (MGT) for *R. fortunei*. In contrast, for *R. vernicosum*, extra Ca^{2+} significantly accelerated the germination speed but had no obvious effects on the final performance and germination uniformity. Extra Ca^{2+} alleviated the negative influence of the alkaline pH on the young seedling performance of *R. fortunei* as shown by the reduced leaf yellowing and lower mortality in both experiments. Given these differential responses, the absorption mechanism of the cations in the three cultivars deserves further investigation. The exogenous application of CaCl_2 also alleviated the heat-induced growth reduction of *Rhododendron* 'Fen Zhen Zhu' [20].

High pH inhibits the uptake of iron and magnesium, both needed for the biosynthesis of chlorophyll and thylakoid proteins, which will result in leaf chlorosis. A high pH in the root apoplast could also restrict Fe^{3+} reductase activity and affect its translocation to the leaves [40]. Demasi et al. [41] showed that in *Rhododendron* spp. Fe deficiency tolerant and sensitive genotypes were distinguishable based on their ferric chelate reductase activity. Leaf chlorosis developed indeed in the alkaline treatments and for all three species (Tables 3 and S2). Furthermore, iron is directly involved in electron transport from PSII to PSI. Alkaline stress will not only affect chloroplast turnover but also induce ROS production which will affect photosynthesis [42]. For the small plantlets in our experiment, chlorophyll *a* fluorescence imaging was an effective tool to detect the negative effects of increased pH on the photosynthetic machinery. When healthy seedlings in the first true leaf stage were transferred to media with increasing pH (Experiment 2), pH stress could already be detected on the second day in the form of a decrease in F_v/F_m and Φ_{PSII} . In addition, in *Lupinus* species, F_v/F_m was lower at pH 8 than at pH 5 and 6.5 [43]. The possibility of high-throughput analysis is one of the essential advantages of CFI, which was created for automatic, faster, and more accurate measurements [26,29,44–46]. In addition, a quantitative image with spatial and temporal information across a sample area in leaves or on the whole plant derived from CFI measurement allows for a more accurate evaluation of the dynamics of (a)biotic stress propagation in an individual sample compared to previous methods [47]. CFI also makes it possible to determine fluorescence kinetics at an early stage at a time when leaves are too small to use portable fluorescence equipment. In this study, the F_v/F_m images and data from CFI show clear variations under high pH stress (Figures 2 and 4), which is useful for CFI-assisted selection of tolerant phenotypes. Additionally, our CFI measurements were conducted without opening the lids of the plantlets' containers, thus maintaining their sterile environment. This allowed for subsequent *in vitro* manipulation and multiplication of selected individuals.

An RGB image analysis system to phenotype the development of *Rhododendron* seedlings and to evaluate the effects of elevated pH on seedling growth was investigated by [48]. In their experiments, seedlings were grown in soilless media with pH levels of 5.7, 7.0, and 7.5 obtained by adding different amounts of CaCO_3 . Seedlings were subsequently photographed to assess the effects of liming treatments on seedling leaf area and leaf hue values. Our CFI method is therefore a more efficient approach, as we were able to monitor the direct effect of the stress treatment on the photosynthetic capacity of the seedling.

Demasi et al. [11] could differentiate 11 *Rhododendron* genotypes in a susceptible, tolerant, and intermediate group by scoring leaf damage, root length variation, and mortality rate of plants in a hydroponic experiment and addition of NaHCO_3 . Preil et al. [34] applied an *in vitro* screening method in a medium with a high concentration of Ca^{2+} and an optimal pH of 5.7 to identify lime-tolerant seedlings in crossing populations of *Rhododendron*. In the current study, we demonstrate that the applications of an *in vitro* screening method in a medium with high pH combined with chlorophyll *a* fluorescence imaging 41 days after sowing allowed us to quickly identify potentially tolerant seedlings. In the seedling populations of the three tested *Rhododendron* species, variation in stress tolerance was observed, and variation increased at higher pH (see Figure 3 for *R. fortunei*). This indicates that genetic variations are present among different species and within the population of specific

species and that selection for pH tolerance might be possible using this high throughput phenotyping method. Despite the potential to select tolerant individuals, our study could not discriminate between the three studied species based on CFI but was able to detect the positive effects of extra Ca^{2+} on F_v/F_m at high pH. Similarly, exogenous Ca^{2+} alleviates photo-inhibition of PSII in peanut leaves during heat stress under high irradiance [49].

5. Conclusions

Acidic and neutral pH do not affect germination kinetics, but alkaline pH results in higher mortality and abnormal leaves. Alkalinity also inhibits the seedling growth of *Rhododendron* species. Exogenous Ca^{2+} can alleviate the negative effects of high pH on seedling mortality in the three studied species but was more effective in suppressing mortality for the alkaline tolerant *R. fortunei*.

Chlorophyll fluorescence imaging is an effective probe for detecting the effects of alkaline stress and Ca on *Rhododendron* seedlings in vitro. High spatial heterogeneity of CFI for small seedlings allows high-throughput screening of tolerant genotypes at an early stage. As the CFI is measured while keeping the seedlings in a sterile environment during the screening process, individual plantlets tolerant to high pH can be easily selected for multiplication. Further studies are needed to understand the effects of exogenous Ca^{2+} on different *Rhododendron* species.

Supplementary Materials: The following supporting information can be downloaded at: <https://www.mdpi.com/article/10.3390/horticulturae8090823/s1>, Figure S1: Germination percentage, development of the cotyledons, abnormal leaves, and true leaves of *R. fortunei* under varying levels of pH and Ca; Table S1: Experiment 3—Overview of pH changes of the medium at the start and the end (day 92) of the experiment; Table S2: Effects of pH and additional 3.4 mM Ca^{2+} on maximum germination (g_{MAX}), mean germination time (MGT), the time between 25% and 75% germination (uniformity) (day 41), percentage of seedlings with open cotyledons (CO) and abnormal cotyledons (AL) (day 61), percentage of seedlings with true leaves (TL) and seedling mortality (day 92), F_v/F_m and Φ_{PSII} on day 41 and day 61 of *R. chihsinianum*, *R. fortunei* and *R. vernicosum*. All values are Mean \pm SE.

Author Contributions: Conceptualization, S.W., L.L., J.V.H. and M.-C.V.L.; methodology, S.W., L.L. and P.L.; formal analysis, S.W.; writing—original draft preparation, S.W.; writing—review and editing, S.W., L.L., P.L., J.V.H. and M.-C.V.L.; supervision, J.V.H. and M.-C.V.L. All authors have read and agreed to the published version of the manuscript.

Funding: This work was supported by the China Scholarship Council (201608360101).

Institutional Review Board Statement: Not applicable.

Informed Consent Statement: Not applicable.

Data Availability Statement: The data presented in this study are available on request from the corresponding author.

Acknowledgments: The authors would like to thank Miriam Levenson for the English language corrections.

Conflicts of Interest: The authors declare no conflict of interest.

References

1. Fang, M.Y.; Fang, R.Z.; He, M.Y.; Hu, L.Z.; Yang, H.B.; Chamberlain, D.F. *Rhododendron*. In *Flora of China*; Wu, Z.Y., Raven, P.H., Hong, D.Y., Eds.; Science Press: Beijing, China; Missouri Botanical Garden Press: St. Louis, LA, USA, 2005; pp. 260–455.
2. Milne, R.I.; Abbott, R.J. Origin and evolution of invasive naturalized material of *Rhododendron ponticum* L. in the British Isles. *Mol. Ecol.* **2000**, *9*, 541–556. [[CrossRef](#)]
3. Zhang, J.-L.; Zhang, C.-Q.; Gao, L.-M.; Yang, J.-B.; Li, H.-T. Natural hybridization origin of *Rhododendron agastum* (Ericaceae) in Yunnan, China: Inferred from morphological and molecular evidence. *J. Plant Res.* **2007**, *120*, 457–463. [[CrossRef](#)]
4. Krebs, S.L. *Rhododendron*. In *Ornamental Crops*; Van Huylbroeck, J., Ed.; Springer: Cham, Switzerland, 2018; pp. 673–718. [[CrossRef](#)]
5. Kinsman, D.J.J. *Rhododendrons* in Yunnan, China—pH of associated soils. *JARS* **1999**, *53*. Available online: <https://scholar.lib.vt.edu/ejournals/JARS/v53n1/v53n1-kinsman.htm> (accessed on 10 August 2022).

6. Lee, J.A.; Woolhouse, H.W. A comparative study of bicarbonate inhibition of root growth in calcicole and calcifuge grasses. *New Phytol.* **1969**, *68*, 1–11. [[CrossRef](#)]
7. Ding, W.; Clode, P.L.; Lambers, H. Is pH the key reason why some *Lupinus* species are sensitive to calcareous soil? *Plant Soil* **2019**, *434*, 185–201. [[CrossRef](#)]
8. Lopez-Bucio, J.; Nieto-Jacobo, M.F.; Ramirez-Rodriguez, V.; Herrera-Estrella, L. Organic acid metabolism in plants: From adaptive physiology to transgenic varieties for cultivation in extreme soils. *Plant Sci.* **2000**, *160*, 1–13. [[CrossRef](#)]
9. M'Sehli, W.; Youssfi, S.; Donnini, S.; Dell'Orto, M.; De Nisi, P.; Zocchi, G.; Abdelly, C.; Gharsalli, M. Root exudation and rhizosphere acidification by two lines of *Medicago ciliaris* in response to lime-induced iron deficiency. *Plant Soil* **2008**, *312*, 151–162. [[CrossRef](#)]
10. Rouphael, Y.; Cardarelli, M.; Di Mattia, E.; Tullio, M.; Rea, E.; Colla, G. Enhancement of alkalinity tolerance in two cucumber genotypes inoculated with an arbuscular mycorrhizal biofertilizer containing *Glomus intraradices*. *Biol. Fertil. Soils* **2010**, *46*, 499–509. [[CrossRef](#)]
11. Demasi, S.; Caser, M.; Kobayashi, N.; Kurashige, Y.; Scariot, V. Hydroponic screening for iron deficiency tolerance in evergreen azaleas. *Not. Bot. Horti Agrobot. Cluj-Napoca* **2015**, *43*, 210–213. [[CrossRef](#)]
12. Hether, N.; Olsen, R.; Jackson, L. Chemical identification of iron reductants exuded by plant roots. *J. Plant Nutr.* **1984**, *7*, 667–676. [[CrossRef](#)]
13. Lee, J.A. The calcicole-calcifuge problem revisited. *Adv. Bot. Res.* **1999**, *29*, 159–167. [[CrossRef](#)]
14. Tyler, G.; Ström, L. Differing Organic Acid Exudation Pattern Explains Calcifuge and Acidifuge Behaviour of Plants. *Ann. Bot.* **1995**, *75*, 75–78. [[CrossRef](#)]
15. Mordhorst, A.P.; Kullik, C.; Preil, W. Ca uptake and distribution in *Rhododendron* selected for lime tolerance. *Gartenbauwissenschaft* **1993**, *58*, 111–116.
16. Giel, P.; Bojarczuk, K. Effects of high concentrations of calcium salts in the substrate and its pH on the growth of selected *Rhododendron* cultivars. *Acta Soc. Bot. Pol.* **2011**, *80*, 105–114. [[CrossRef](#)]
17. Clapham, D.E. Calcium signaling. *Cell* **2007**, *131*, 1047–1058. [[CrossRef](#)]
18. Wilkins, K.A.; Matthus, E.; Swarbreck, S.M.; Davies, J.M. Calcium-mediated abiotic stress signaling in roots. *Front. Plant Sci.* **2016**, *7*, 1296. [[CrossRef](#)]
19. Kerchev, P.; van der Meer, T.; Sujeeth, N.; Verlee, A.; Stevens, C.V.; Van Breusegem, F.; Gechev, T. Molecular priming as an approach to induce tolerance against abiotic and oxidative stresses in crop plants. *Biotechnol. Adv.* **2020**, *40*, 107503. [[CrossRef](#)]
20. Shen, H.; Zhao, B.; Xu, J.; Zheng, X.; Huang, W. Effects of Salicylic Acid and Calcium Chloride on Heat Tolerance in *Rhododendron* 'Fen Zhen Zhu'. *J. Am. Soc. Hortic. Sci.* **2016**, *141*, 363–372. [[CrossRef](#)]
21. Li, T.; Liu, X.; Li, Z.; Ma, H.; Wan, Y.; Liu, X.; Fu, L. Study on Reproductive Biology of *Rhododendron longipedicellatum*: A Newly Discovered and Special Threatened Plant Surviving in Limestone Habitat in Southeast Yunnan, China. *Front. Plant Sci.* **2018**, *9*, 33. [[CrossRef](#)]
22. Wang, S.; Leus, L.; Van Labeke, M.-C.; Van Huylenbroeck, J. Prediction of Lime Tolerance in *Rhododendron* Based on Herbarium Specimen and Geochemical Data. *Front. Plant Sci.* **2018**, *9*, 1538. [[CrossRef](#)]
23. Milne, R.I.; Davies, C.; Prickett, R.; Inns, L.H.; Chamberlain, D.F. Phylogeny of *Rhododendron* subgenus *Hymenanthes* based on chloroplast DNA markers: Between-lineage hybridisation during adaptive radiation? *Oesterreichische Bot. Z.* **2010**, *285*, 233–244. [[CrossRef](#)]
24. Ashraf, M.; Foolad, M.R. Pre-Sowing Seed Treatment—A Shotgun Approach to Improve Germination, Plant Growth, and Crop Yield Under Saline and Non-Saline Conditions. *Adv. Agron.* **2005**, *88*, 223–271. [[CrossRef](#)]
25. Li, H.; Zhang, D. In Vitro Seed Germination of *Kalmia latifolia* L. Hybrids: A Means for Improving Germination and Speeding Up Breeding Cycle. *HortScience* **2018**, *53*, 535–540. [[CrossRef](#)]
26. Harbinson, J.; Prinzenberg, A.E.; Kruijer, W.; Aarts, M.G. High throughput screening with chlorophyll fluorescence imaging and its use in crop improvement. *Curr. Opin. Biotechnol.* **2012**, *23*, 221–226. [[CrossRef](#)] [[PubMed](#)]
27. Esong, X.; E Zhou, G.; Xu, Z.; Elv, X.; Ewang, Y. Detection of Photosynthetic Performance of *Stipa bungeana* Seedlings under Climatic Change using Chlorophyll Fluorescence Imaging. *Front. Plant Sci.* **2016**, *6*, 1254. [[CrossRef](#)]
28. Li, H.; Wang, P.; Weber, J.F.; Gerhards, R. Early identification of herbicide stress in soybean (*Glycine max* (L.) Merr.) using chlorophyll fluorescence imaging technology. *Sensors* **2018**, *18*, 21. [[CrossRef](#)]
29. Mishra, K.B.; Mishra, A.; Novotna, K.; Rapantova, B.; Hodanova, P.; Urban, O.; Klem, K. Chlorophyll a fluorescence, under half of the adaptive growth-irradiance, for high-throughput sensing of leaf-water deficit in *Arabidopsis thaliana* accessions. *Plant Methods* **2016**, *12*, 46. [[CrossRef](#)]
30. Pieczywek, P.; Cybulska, J.; Szymanska-Chargot, M.; Siedliska, A.; Zdunek, A.; Nosalewicz, A.; Baranowski, P.; Kurenda, A. Early detection of fungal infection of stored apple fruit with optical sensors—Comparison of biospeckle, hyperspectral imaging and chlorophyll fluorescence. *Food Control* **2018**, *85*, 327–338. [[CrossRef](#)]
31. Sun, D.; Zhu, Y.; Xu, H.; He, Y.; Cen, H. Time-Series Chlorophyll Fluorescence Imaging Reveals Dynamic Photosynthetic Fingerprints of sos Mutants to Drought Stress. *Sensors* **2019**, *19*, 2649. [[CrossRef](#)]
32. Anderson, W.C. A Revised Tissue Culture Medium for Shoot Multiplication of *Rhododendron*. *J. Am. Soc. Hortic. Sci.* **1984**, *109*, 343–347. [[CrossRef](#)]

33. Joosen, R.V.L.; Kodde, J.; Willems, L.A.J.; Ligterink, W.; van der Plas, L.H.W.; Hilhorst, H.W. GERMINATOR: A software package for high-throughput scoring and curve fitting of *Arabidopsis* seed germination. *Plant J.* **2010**, *62*, 148–159. [[CrossRef](#)]
34. Preil, W.; Ebbinghaus, R. Breeding of lime tolerant *Rhododendron* rootstocks. *Acta Hort.* **1994**, *364*, 61–70. [[CrossRef](#)]
35. McAleese, A.J.; Rankin, D.W.H. Growing rhododendrons on limestone soils: Is it really possible? *JARS* **2000**, *54*, 126–134. Available online: <https://scholar.lib.vt.edu/ejournals/JARS/v54n3/v54n3-mcaleese.html> (accessed on 10 August 2022).
36. Shujun, Y.U.; Ximing, C.; Jeongsik, L.E.E. Alkali tolerance of *Rhododendron fortunei* in subirrigated ebb & flow bench systems with hydroponics. *Acta Hort. Sin.* **2008**, *35*, 715–720.
37. Chaanin, A. Lime tolerance in rhododendron. *Comb. Proc. IPPS* **1998**, *48*, 180–182.
38. Yu, S.; Hou, Y.; Zhang, Y.; Guo, W.; Xue, Y. Contrasting Effects of NaCl and NaHCO₃ Stresses on Seed Germination, Seedling Growth, Photosynthesis, and Osmoregulators of the Common Bean (*Phaseolus vulgaris* L.). *Agronomy* **2019**, *9*, 409. [[CrossRef](#)]
39. Guo, R.; Yang, Z.; Li, F.; Yan, C.; Zhong, X.; Liu, Q.; Xia, X.; Li, H.; Zhao, L. Comparative metabolic responses and adaptive strategies of wheat (*Triticum aestivum*) to salt and alkali stress. *BMC Plant Biol.* **2015**, *15*, 170. [[CrossRef](#)]
40. Kosegarten, H.; Koyro, H.-W. Apoplastic accumulation of iron in the epidermis of maize (*Zea mays*) roots grown in calcareous soil. *Physiol. Plant.* **2001**, *113*, 515–522. [[CrossRef](#)]
41. Demasi, S.; Handa, T.; Scariot, V. Ferric chelate reductase activity under iron deficiency stress in Azalea. *Int. J. Hort. Floricult.* **2015**, *3*, 157–160.
42. Marschner, H. *Mineral Nutrition of Higher Plants*, 2nd ed.; Academic Press: London, UK, 1995; pp. 641–657.
43. Ding, W.; Clode, P.L.; Lambers, H. Effects of pH and bicarbonate on the nutrient status and growth of three *Lupinus* species. *Plant Soil* **2020**, *447*, 9–28. [[CrossRef](#)]
44. Rousseau, C.; Belin, E.; Bove, E.; Rousseau, D.; Fabre, F.; Berruyer, R.; Guillaumes, J.; Manceau, C.; Jacques, M.A.; Boureau, T. High throughput quantitative phenotyping of plant resistance using chlorophyll fluorescence image analysis. *Plant Methods* **2013**, *9*, 17. [[CrossRef](#)] [[PubMed](#)]
45. Tschiersch, H.; Junker, A.; Meyer, R.C.; Altmann, T. Establishment of integrated protocols for automated high throughput kinetic chlorophyll fluorescence analyses. *Plant Methods* **2017**, *13*, 54. [[CrossRef](#)] [[PubMed](#)]
46. Wang, H.; Qian, X.; Zhang, L.; Xu, S.; Li, H.; Xia, X.; Dai, L.; Xu, L.; Yu, J.; Liu, X. A Method of High Throughput Monitoring Crop Physiology Using Chlorophyll Fluorescence and Multispectral Imaging. *Front. Plant Sci.* **2018**, *9*, 407. [[CrossRef](#)]
47. Sekulska-Nalewajko, J.; Kornas, A.; Goclawski, J.; Miszalski, Z.; Kuzniak, E. Spatial referencing of chlorophyll fluorescence images for quantitative assessment of infection propagation in leaves demonstrated on the ice plant: *Botrytis cinerea* pathosystem. *Plant Methods* **2019**, *15*, 18. [[CrossRef](#)]
48. Susko, A.; Rinehart, T.A.; Bradeen, J.; Hokanson, S.C. An Evaluation of Two Seedling Phenotyping Protocols to Assess pH Adaptability in Deciduous Azalea (*Rhododendron* sect. *Pentanthera* G. Don). *HortScience* **2018**, *53*, 268–274. [[CrossRef](#)]
49. Yang, S.; Wang, F.; Guo, F.; Meng, J.-J.; Li, X.-G.; Dong, S.-T.; Wan, S.-B. Exogenous Calcium Alleviates Photoinhibition of PSII by Improving the Xanthophyll Cycle in Peanut (*Arachis Hypogaea*) Leaves during Heat Stress under High Irradiance. *PLoS ONE* **2013**, *8*, e71214. [[CrossRef](#)] [[PubMed](#)]